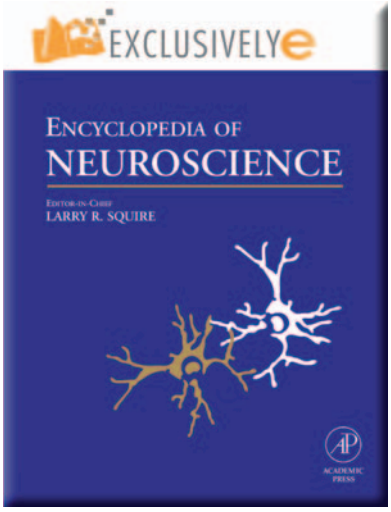

Gruetter R (2009) Glial Energy Metabolism: A NMR Spectroscopy Perspective. In: Squire LR (ed.) Encyclopedia of Neuroscience, volume 4, pp. 773-781. Oxford: Academic Press.

Glial Energy Metabolism: A NMR Spectroscopy Perspective

R Gruetter, Ecole Polytechnique Fédérale de Lausanne, University of Lausanne, Lausanne-Geneva, Switzerland

Introduction

During increased electrical brain activity, blood flow increases, tissue deoxyhemoglobin content decreases, glucose metabolism increases, and possibly oxygen metabolism increases. These changes in metabolism and the hemodynamic consequences are measured with contemporary brain imaging methods. However, the measurement of brain activity, be it through the hemodynamic correlates of increased electrical activity, increased oxygen consumption, or deoxyglucose uptake, is unable to depict the fundamentals of brain activity at the neuroglial level *in vivo*. The major mechanism of deactivation of the major excitatory neurotransmitter, glutamate, is glial uptake and conversion to electrophysiologically inactive glutamine, which is then transported back to the neuron to replenish the neurotransmitter pool of glutamate, completing the glutamate–glutamine cycle. It is the purpose of this article to summarize perspectives on *in vivo* metabolism in the glial compartment, relative to that in the neuronal compartment, that have been gained using an emerging method, namely nuclear magnetic resonance (NMR) spectroscopy. Most measurements are performed at metabolic steady state, defined as a condition of metabolic fluxes being constant.

NMR Spectroscopy of Brain Energy Metabolism: A Brief Primer

NMR spectroscopy of brain energy metabolism has focused chiefly on the signals from three NMR-active nuclei – the ubiquitously used ^{1}H, as well as ^{31}P and ^{13}C. Of the three, ^{1}H and ^{31}P are 100% naturally abundant, whereas ^{13}C is only 1.1% abundant in nature. Techniques to establish the quantitative measurement of energy metabolism depend critically on the specific signal measured from a given nucleus. In the following discussions, the current state-of-the-art measurements are given, without elaborating on methodological considerations in detail.

Proton NMR Spectroscopy

With suppression of the intense signal of water, which is used for magnetic resonance imaging (MRI), and elimination of the extracerebral fat signal by adequate localization, a multitude of resonances can be observed in the *in vivo* ^{1}H NMR spectrum; these are attributed to date to more than 20 compounds that can be quantitated with typical precision of ~10%, amounting to a neurochemical profile (Figure 1). Quantification is typically achieved by referencing the metabolite signal to an internal reference signal of known concentration, such as water. Metabolic rates are typically either inferred from measured metabolite concentrations or from their changes with time.

Phosphorus NMR Spectroscopy

The *in vivo* signal of the ^{31}P nucleus contains signals from the three phosphates of ATP – signals from inorganic phosphate and phosphocreatine, as well as signals attributed to phosphomonoester compounds, such as phosphoethanolamine and phosphocholine, and signals attributed to phosphodiesters, such as glycerophosphocholine and ethanolamine. The signals of ADP and UDP-glucose are in principle observable but are typically too low to be detected. The chemical shift of inorganic phosphate reveals intracellular pH, and by manipulating the magnetization of inorganic phosphate, phosphocreatine, or the γ-phosphate of ATP through magnetization transfer, the rates of the reactions of creatine kinase or ATPase can be assessed. Quantification is typically achieved by referencing relative to a brain ATP concentration of 3 mM.

Carbon-13 NMR Spectroscopy

The sensitivity of ^{13}C NMR spectroscopy can be improved by administering ^{13}C-labeled precursors, such as glucose, lactate, β-hydroxybutyrate, or acetate. Further sensitivity improvements are possible by indirectly detecting the ^{13}C label through vicinal ^{1}H nuclei. As in radiotracer methods, such as positron emission tomography (PET), the measurement of label incorporation into metabolic products allows the determination of metabolic rates using similar mathematical approaches. Energy metabolism has been assessed from the measurement of brain glucose, glycogen, lactate, glutamate, glutamine, and aspartate (Figure 2). Quantification is typically achieved by performing an external reference measurement.

Glycolysis

Glucose Transport

The brain relies on a continuous import of glucose from the blood across the blood–brain barrier. Glucose transport rates into the brain are thus indicative of the maximal sustainable rate of glucose consumption,

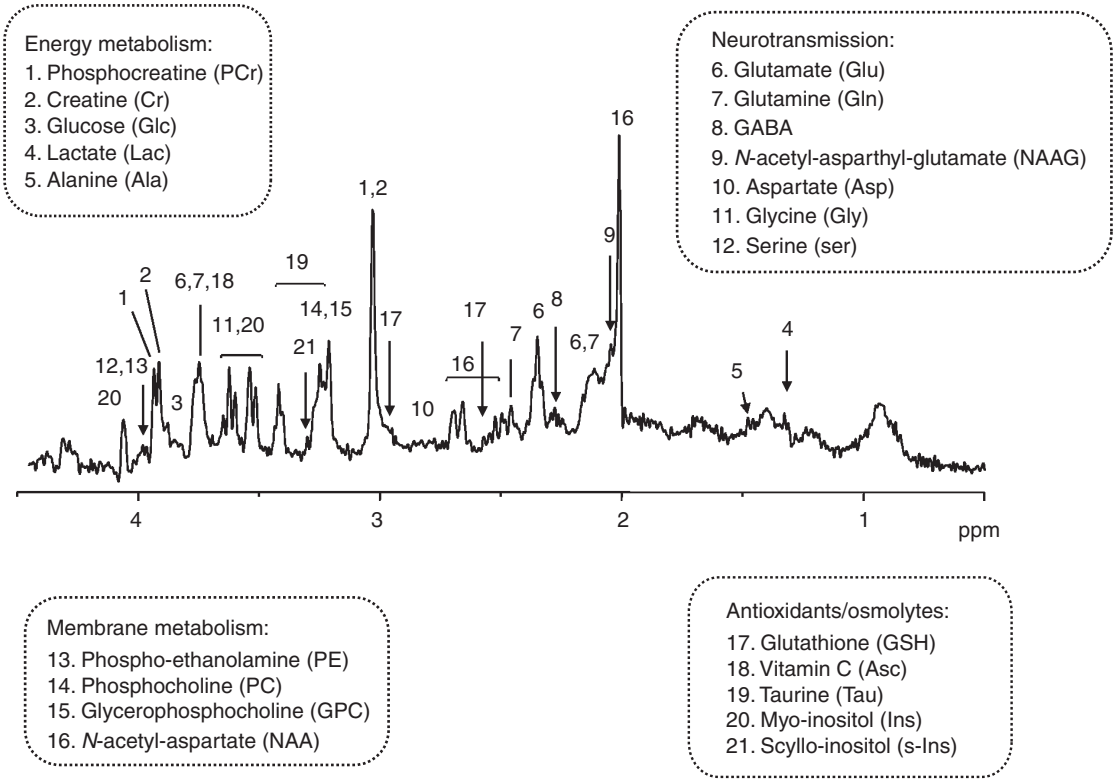

Figure 1 A neurochemical profile can be derived from the proton nuclear magnetic resonance spectrum of the brain (TE = 2.7 ms, 9.4 T). Shown are 21 compounds that can be measured *in vivo*, grouped according to their major significance. In addition, when present, acetate and β-hydroxybutyrate can also be measured.

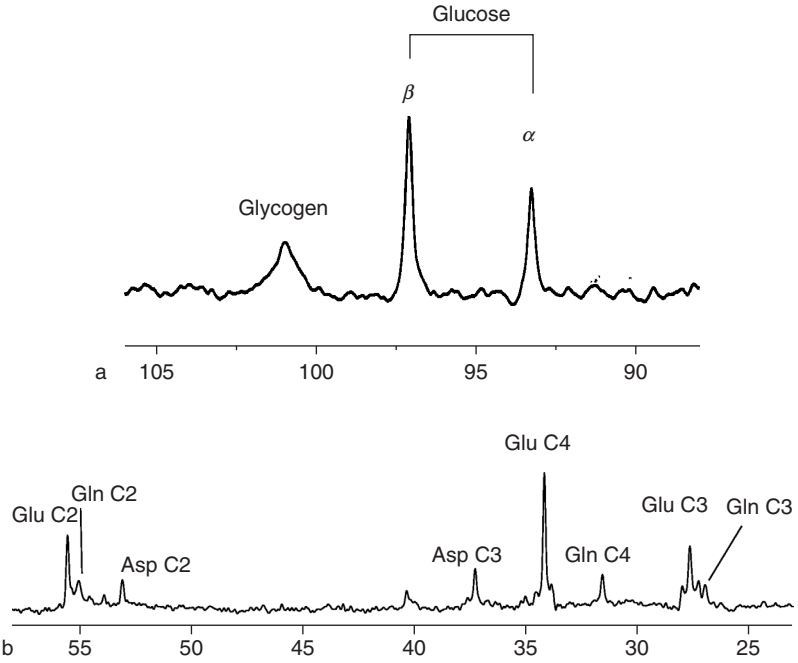

Figure 2 (a) Localized ^{13}C nuclear magnetic resonance spectroscopy of the C1 of glucose and glycogen in rat brain (9.4 T). (b) Localized ^{13}C nuclear magnetic resonance spectroscopy of the human brain (4 T). Spectra in both panels are shown after [1–^{13}C]glucose administration. Label incorporation is observed in the predominantly neuronal glutamate and aspartate and the predominantly glial glutamine, in multiple positions due to label scrambling in the tricarboxylic acid cycle, and exchange with cytosolic amino acids due to, for example, the action of the malate–aspartate shuttle.

CMR_{glc}. Knowledge of the size of the brain glucose pool is important for the derivation of absolute metabolic fluxes and quantitative positron emission tomography studies. Steady-state glucose transport kinetics can be derived from the relationship between brain and plasma glucose. The former can be directly measured using NMR spectroscopy.

Brain glucose is distributed in the entire aqueous phase of the brain The volume in the brain into which glucose diffuses (i.e., the physical distribution volume, V_d) is critical in the derivation of glucose transport kinetics. The diffusion behavior of glucose, measured by diffusion-weighted NMR spectroscopy, reflects that ~80% of the glucose in brain tissue is intracellular, consistent with a high physical distribution volume for glucose, $V_d = 80\%$, which is approximately equal to the brain's water phase. Intracellular and extracellular glucose concentrations are approximately equal, suggesting that transport of glucose across the cell membranes is fast compared to the glucose consumption rate. Conversely, the limiting step for glucose entry into the brain is at the blood–brain barrier (BBB), comprising the endothelial cells.

Glucose content reflects the balance between transport and consumption The steady-state brain glucose concentration is a sensitive indicator of the ability of the BBB to transport glucose relative to the rate of glucose consumption, T_{max}/CMR_{glc}. The observed linear relationship between plasma and brain glucose is consistent with the need to take into account the reversibility of the transport process (Figure 3). The apparent K_m of glucose transport, K_t, is of the order of 5 mM. Decreased electrical activity and thus decreased energy metabolism result in increased brain glucose concentrations; yet a sizable concentration gradient is maintained at isoelectricity, implicating considerable net glucose uptake and thus substantial energy metabolism not related to signaling (Figure 4(a)). Increases in luminal glucose transporter (GLUT-1) result in an increase in the maximal transport capacity of the BBB, the consequence of which is an accordingly increased brain glucose content, suggesting that the luminal membrane is the major rate-determining step for glucose entry into the brain (Figure 4(b)).

Brain glucose becomes rate limiting for metabolism when its concentration approaches that of the K_m of the first step in its metabolism, which in the brain is

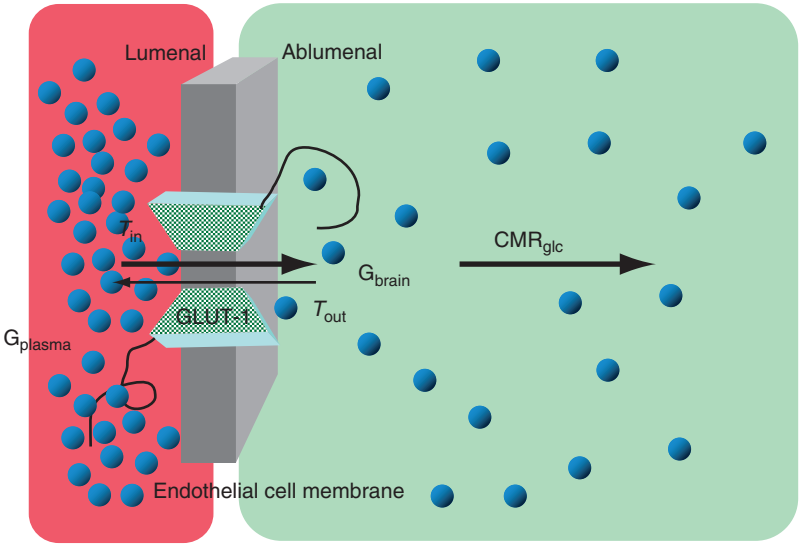

$$T_{in} = T_{out} + CMR_{glc}$$

$$T_{in} = T_{max} \frac{G_{plasma}}{(K_t + G_{brain}/V_d) + G_{plasma}} \qquad T_{out} = T_{max} \frac{G_{brain}}{(K_t + G_{plasma})V_d + G_{brain}}$$

Figure 3 Schematic of glucose (G) transport across the blood–brain barrier, depicting the steady-state situation and showing the reversible Michaelis–Menten kinetic expression for transport (CMR_{glc}, maximal sustainable rate of glucose consumption). Standard Michaelis–Menten kinetics neglect the effect of product concentration on reaction velocity (V), and expressions for the transport rates (T_{in} and T_{out}) are derived by assuming zero product concentration (i.e., by setting $G_{brain} = 0$ for T_{in} and $G_{plasma} = 0$ for T_{out}).

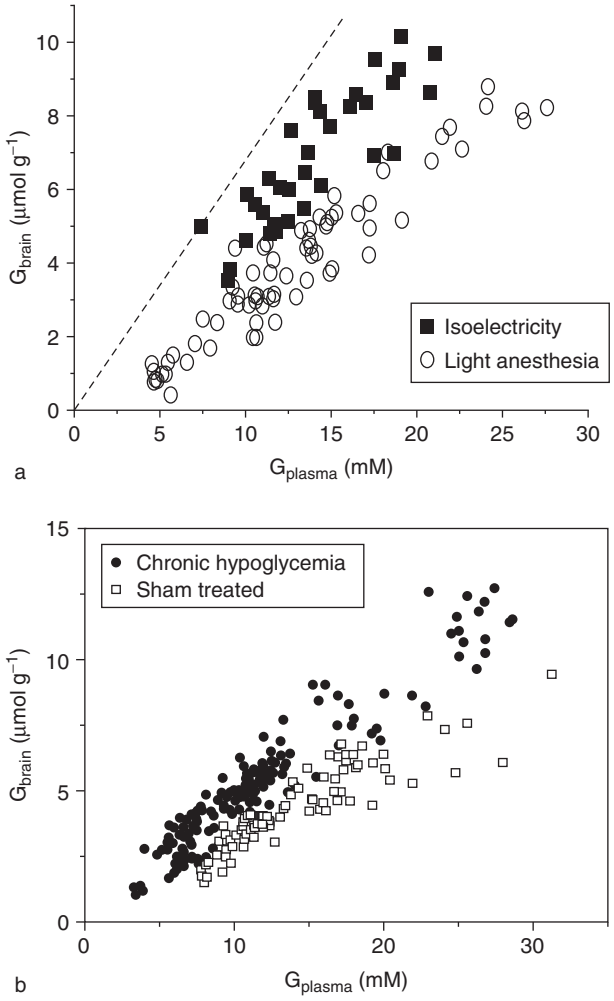

Figure 4 (a) Effect of reduced brain activity on brain glucose concentration in the rat brain. Reduction of electrical activity increases brain glucose content substantially, but a considerable gradient across the blood–brain barrier is maintained (the dashed line indicates the G_{brain}:G_{plasma} relationship in the absence of a gradient). (b) Effect of 50% increased blood–brain barrier glucose transporter GLUT-1 on brain glucose content. GLUT-1 was increased by inducing chronic hypoglycemia, which led to a substantial increase in brain glucose content at a constant brain glucose consumption rate.

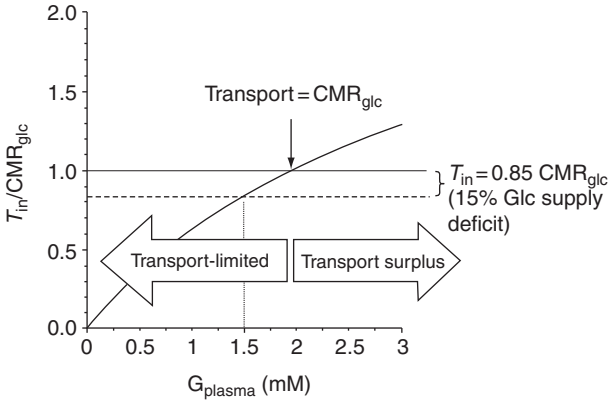

Figure 5 Glucose transport can become rate limiting for metabolism, but this is a gradually increasing deficit. The graph shows the unidirectional glucose influx rate, T_{in}, relative to the glucose consumption rate, CMR_{glc}. In this example glucose influx matches the consumption at $G_{plasma} \sim 2$ mM. As a result, even at substantial hypoglycemia (e.g., $G_{plasma} = 1.5$ mM), the glucose supply (i.e., T_{in}) accounts for ~85% of total glucose requirements.

mostly phosphorylation by hexokinase. Since the K_m of brain hexokinase is very low (~50 μM), brain glucose concentrations that are close to zero indicate metabolism that is limited by the glucose available to the brain cell (transport-limited metabolism). The substantial brain glucose content at euglycemia indicates that brain glucose transport is not rate limiting for metabolism under normal circumstances; the maximal sustainable rate of glucose consumption is approximately two to three times above the basal rate of glucose metabolism. Glucose consumption can, however, transiently exceed the maximum unidirectional transport into the brain, which may occur in conditions of extreme metabolic activation, such as during seizures. While plasma glucose drops, the brain traverses from excess glucose supply to a condition in which transport across the BBB supplies just enough glucose for metabolism, and eventually to a gradually increasing deficit in glucose supply (Figure 5).

During hypoglycemia, glucose metabolism tends to decrease and cerebral blood flow (CBF) increases when the brain glucose concentration approaches the K_m of hexokinase. The mechanism of such blood flow regulation is different from the neurovascular coupling in physiological activation, whereby glucose metabolism and CBF increase concomitantly.

Glial Glycogen – The Only Energy Reserve in Brain

Glycogen, ascribed to the glial compartment, is present in concentrations that exceed those of euglycemic brain glucose by severalfold. It thus comprises by far the most concentrated endogenous storage of glucose equivalents in the central nervous system (CNS), and the presence of glycogen stores is essential for brain function. Similar to glucose, brain glycogen is rapidly eliminated postmortem; therefore, its direct biochemical measurement is difficult. Localized ^{13}C NMR spectroscopy has the unique capability of following brain glycogen metabolism longitudinally, allowing measurement of the rate of change of metabolic rates and concentration changes of glycogen.

Brain glucose can regulate glycogen metabolism Glycogen metabolism in brain accounts for only a few percent of total glucose metabolism under resting conditions. In contrast to transport and metabolism of bulk brain glucose, glycogen metabolism is strongly insulin dependent and to a lesser degree its content

depends on the plasma glucose concentration. In deep anesthesia and hyperglycemia – conditions which are associated with increased brain glucose content – brain glycogen levels rise well above the normal concentration. Together with the apparent stability of glycogen in the nonstimulated brain at euglycemia or hyperglycemia, these data suggest that brain glucose plays an important regulatory role in cerebral glycogenolysis.

When the intracellular glucose concentration approaches the K_m of hexokinase, glycogen phosphorylase is activated and glycogen synthase is deactivated, resulting in net glycogenolysis to glucose-6-phosphate (and some free glucose, due to cleavage of the 1–6 bonds in glycogen by the debranching enzyme). Glucose-6-phosphate is eventually metabolized to pyruvate, which can either enter the tricarboxcylic acid (TCA) cycle or be converted by lactate dehydrogenase to lactate. Glial lactate can be exported via the action of monocarboxylate transporters at the glial and neuronal cell membranes.

Glycogen stores are neuroprotective By providing lactate to the extracellular fluid, astrocytes can sustain neuronal energy metabolism of neighboring neurons in conditions of fuel deprivation, such as hypoglycemia. During glycogenolysis, two ATPs per glucosyl unit are generated in glycolysis, which can provide energy to support uptake of synaptic glutamate and conversion into electrophysiologically inactive glutamine. Astrocytes thus can remove excitotoxic glutamate from the synaptic cleft in energy-deprived situations, which may be one mechanism by which glial glycogen exerts its neuroprotective effect (Figure 6).

Following glycogen depletion, be it induced by neurotransmitters, by hypoglycemia, by hypoxia, or by sleep deprivation, brain glycogen increases above the basal level and beyond in the presence of ample insulin and glucose, resulting in 'supercompensation' similar to that observed for glycogen in noncerebral tissues. Increased astrocytic glycogen levels reduce neuronal damage following subsequent fuel deprivation. Brain glycogen metabolism may be a factor involved in the mechanism of the hypoglycemia unawareness syndrome observed clinically in patients with insulin-treated diabetes, probably through the enhanced neuroprotective effect of increased brain glycogen.

Glycogen is an important energy reserve Glycogen serves as an energy reservoir of glucose equivalents.

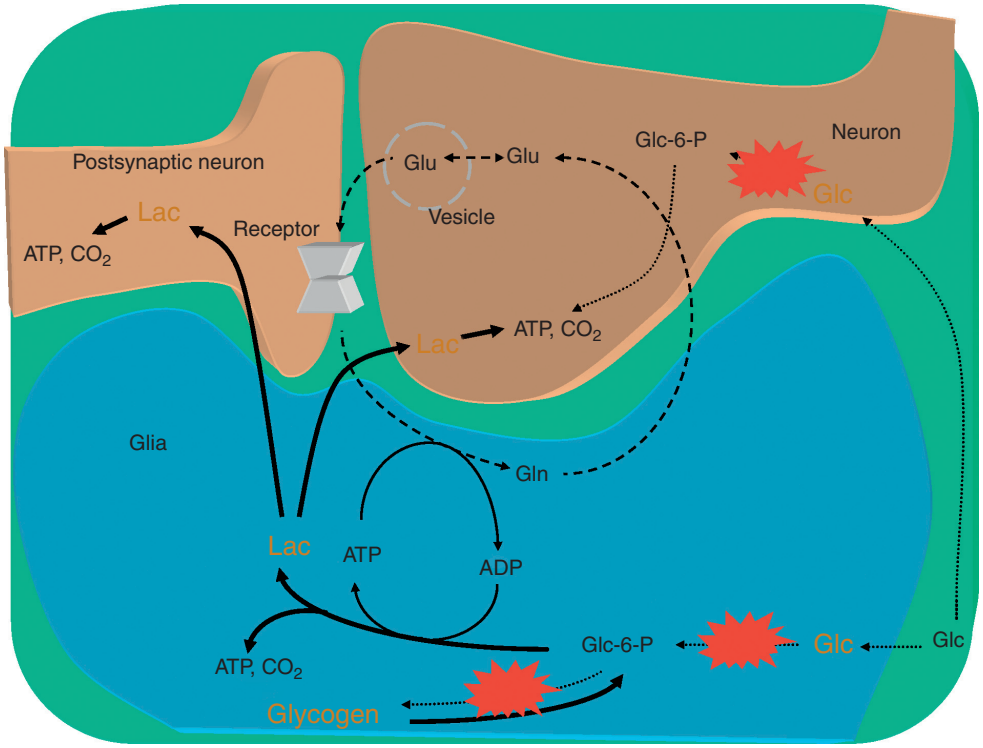

Figure 6 Schematic showing the neuroprotective role of glial glycogen and its ability to nourish neighboring neurons with substrates, such as lactate (Lac). In glucoprivation, such as hypoglycemia, glucose phosphorylation impaired, leading to insufficient glucose-6-phosphate (Glc-6-P) generation, deactivated glycogen synthase (red stars), and activated glycogen phosphorylase. The ensuing glycogen breakdown, through its metabolic pathways (solid thick lines), ultimately produces fuel for neighboring neurons. Glial glycogen is probably also neuroprotective through its ability to minimize excitotoxicity by providing energy for removal of glutamate from the synaptic cleft in fuel-deprived conditions.

For example, during aglycemia, when the supply of glucose to the brain cells is completely abolished, glycogen would sustain total glucose metabolism for about 20 min. However, aglycemia is difficult to achieve in the living brain, and the reduction of plasma glucose in reality is gradual in time, resulting in a gradually increasing glucose supply deficit (Figure 5). For example, in order to cover a partial supply deficit of the metabolic rate of glucose of 0.05 μmol g^{-1} min^{-1} in the awake human brain (corresponding to a deficit of 14% of a basal metabolic rate of 0.35 μmol glucose g^{-1} min^{-1}), the cerebral content of glycogen of 3.5 μmol glucosyl units g^{-1} can account for this fuel deficit for more than 1 h. The rate of brain glycogen degradation during hypoglycemia accounts for the majority of the glucose supply deficit during the hypoglycemic period, and following extended periods of moderate hypoglycemia, substantial glycogen reserves remain. The time estimated for complete glycogen depletion is 4 h, which corresponds to the time period that clinically results in residual neurological symptoms after an episode of hypoglycemia.

In chronic hypoglycemia, brain glucose content is elevated (Figure 4(b)), resulting in ambient intracellular glucose content that appears normal, despite the prevalent hypoglycemia. In this condition, consistent with the upregulation of brain glucose content, astrocytic 45 kDa GLUT-1 and neuronal GLUT-3 are unaltered, as are brain glycogen concentrations.

Glycogen is an important store of glucose equivalents in the brain, having a significant neuroprotective effect; glycogen metabolism is affected not only by tissue glucose levels and plasma insulin, but also by other hormones, neurotransmitters, and second messengers.

Lactate Metabolism – An Integral Part of Normal Brain Function

Brain lactate is present at near 1 μmol g^{-1} concentration under normoxic conditions *in vivo*, and is continuously synthesized and broken down. Glucose and glycogen are the major metabolic precursors for lactate, which can be exported and serve as fuel for other cells. A small lactate efflux from the brain is observed normally. Rapid but small increases in brain lactate are observed in focal activation, consistent with a transient uncoupling of oxygen and glucose metabolism. Similar to that for glucose, lactate diffusion behavior is restricted, indicating that most tissue lactate is intracellular. Lactate is almost evenly distributed in the brain's aqueous phase, owing to the large transport capacity of the abundant monocarboxylate transporters at the neuronal and glial cell membranes.

Tricarboxylic Acid Cycles

Glutamate Turnover – How Oxygen Metabolism Is Measured by NMR Spectroscopy

When using a substrate labeled at a suitable position, be it glucose or other suitable substrates, the measurement of oxygen metabolism by NMR spectroscopy can be accomplished by measuring the rate of labeling of glutamate. For simplicity we consider glucose labeled at the 1 and 6 positions, which labels the C3 of pyruvate and ultimately the C2 of acetyl-CoA, which condenses with oxaloacetate to form citrate. In the course of the metabolic reactions of the TCA cycle, which occur at a rate denominated as V_{TCA}, label arrives at the C4 of 2-oxoglutarate. Oxoglutarate is exchanged with glutamate through transamination and thus readily labels mitochondrial glutamate. However, in the brain *in vivo*, most of the tissue glutamate is of cytosolic origin, given the small volume fraction occupied by mitochondria. Therefore, when label incorporation into glutamate is observed, it reflects a signal ascribed mainly to the cytosol (Figure 7(a)). The label scrambling, however, occurs in the mitochondria. Carbon-13 label is transferred to the cytosolic glutamate by label exchange across the inner mitochondrial membrane. Processes such as the malate–aspartate shuttle (Figure 7(b)), which transfer reducing equivalents from the cytosol to the mitochondrion, play a key role in label exchange across the mitochondrial membrane. Therefore, the rate of labeling of glutamate is both a function of the TCA cycle rate (V_{TCA}) as well as of isotope exchange across the inner mitochondrial membrane (V_x).

When considering the further fate of label in the C4 of glutamate (and conversely the C4 of 2-oxoglutarate), the investigational power of NMR spectroscopy can be demonstrated. The label at C4 of 2-oxoglutarate proceeds along the TCA cycle to scramble equally between the C2 and C3 of succinate (a symmetric molecule), which ultimately leads to a symmetric labeling of the C2 and C3 of 2-oxoglutarate and thus by the same exchange mechanism (V_x in Figure 7(a)) the C2 and C3 of glutamate. Hence, as a result of metabolic reactions ascribed to the TCA cycle, label from a singly labeled acetyl-CoA molecule results in labeling of glutamate in three positions in two turns of the TCA cycle. Whereas the labeling of the C4 of glutamate takes up a simple analytical form of an exponential function, the rate of which is the geometric average of V_{TCA} and V_x divided by the glutamate pool size, the labeling of the C2 and C3 of glutamate is more complex. Briefly, at the C3 position, glutamate receives label not only from acetyl-CoA, but since some of the label escapes the oxoglutarate pool into glutamate (with a probability determined by the relative rate of V_{TCA} and V_x), its C4 position increasingly serves as

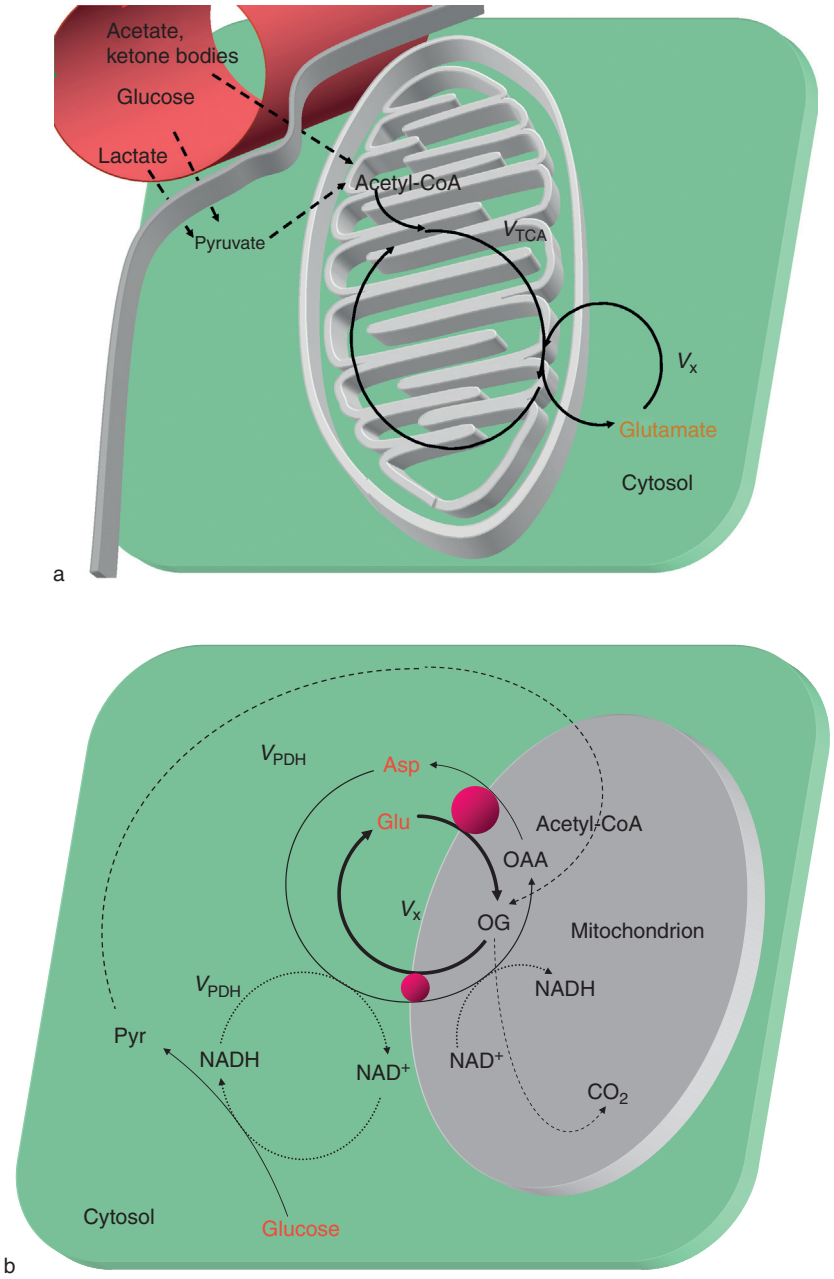

Figure 7 The flow of label from glucose to glutamate: (a) illustration of the flow of label from acetyl-CoA to glutamate; (b) the metabolic reactions involved in the malate–aspartate shuttle. The malate–aspartate (Asp) shuttle allows the cell to combust glucose oxidatively, by transferring the reducing equivalent generated per pyruvate (Pyr) molecule oxidized to the mitochondrion. This shuttle is critical in permitting respiring neural cells to metabolize glucose. When pyruvate is the sole fuel for the tricarboxylic acid (TCA) cycle, the TCA cycle rate $V_{TCA} = V_{PDH}$ (PDH, pyruvate dehydrogenase; V_x, isotope exchange across the inner mitochondrial membrane; OG, oxoglutarate; OAA, oxaloacetic acid).

label substrate for the C3. Since the rate of labeling of Glu_4 is delayed compared to that of acetyl-CoA, due to the time required to completely label the glutamate pool, the labeling of Glu_3 is an increasingly concave function when increasing transmitochondrial exchange rate V_x, which thus can be assessed, allowing important insights into the regulation of oxidative metabolism and mitochondrial integrity *in vivo*. The labeling of glutamate by itself does not permit to study compartmentalization between astrocytes and neurons, however, as glutamate is ubiquitously present in many cells, including astrocytes.

The Glutamate–Glutamine Cycle

Glial-specific tracers Acetate and glucose do not share the same product-precursor relationship.

Today it is well established that acetate is selectively taken up by astrocytes, and hence labeled acetate can be used to 'trace' glial metabolism, whether it is by using radiotracers, as in ^{14}C autoradiography or ^{11}C (using PET), or by using [^{13}C]acetate in conjunction with NMR spectroscopy. The advantage of using acetate as a tracer lies in its exclusive uptake into the astrocytes, and thus from the turnover of glutamate, astrocytic TCA cycle flux can be assessed.

Labeled acetate will thus label glial glutamate much in the same manner as discussed previously; however, the action of glutamine synthetase and the diffusion of glutamine from the astrocyte into the presynaptic terminal result in label being scrambled from glutamine to neuronal glutamate, where it is being diluted with unlabeled carbon derived from the neuronal TCA cycle; this leads to a lower isotopic enrichment of tissue glutamate, compared to tissue glutamine (resulting in an anomalous product-precursor relationship). In general, glutamate and glutamine are not labeled to an equal extent, reflecting the substantial activity of the glial TCA cycle (see later).

When electrical activity ceases (isoelectricity) the glutamate–glutamine cycle activity is close to zero, but substantial energy is still expended, powering ion gradients, among others. This results in a substantial glucose concentration gradient at isoelectricity and active oxygen consumption (Figure 4(a)). With increasing electrical activity, the rate of glutamine synthesis increases but the glutamate–glutamine cycle does not operate stoichiometrically.

Glutamine Synthetase and Pyruvate Carboxylase

The synthesis of glutamine is catalyzed by glutamine synthetase (EC 6.3.1.2), which is attributed to the glial compartment (Figure 8). Hence the *in vivo* observation of glutamine labeling by ^{13}C NMR is a direct manifestation of glial metabolism. In principle, the simultaneous observation of labeling of glutamate, mainly ascribed to the neuronal compartment, and glutamine, a glial reaction, would thus follow the path of acetyl-CoA → glutamate → glutamine → glutamate, and thus would represent a direct manifestation of the glutamate–glutamine cycle, which is the dominant mechanism of glutamate neurotransmission. However, additional labeling of glutamine occurs via the glial TCA cycle, as astrocytes contain mitochondria and thus the necessary enzymatic predisposition for oxidative generation of energy (e.g., a high cytochrome oxidase content).

The presence of significant glial oxidative metabolism results in incorporation into glutamine label that does not match that of glutamate. Reactions associated with CO_2 fixation, such as the major anaplerotic enzyme, pyruvate carboxylase (EC 6.4.1.1), have been localized to astrocytes. *De novo* synthesis of

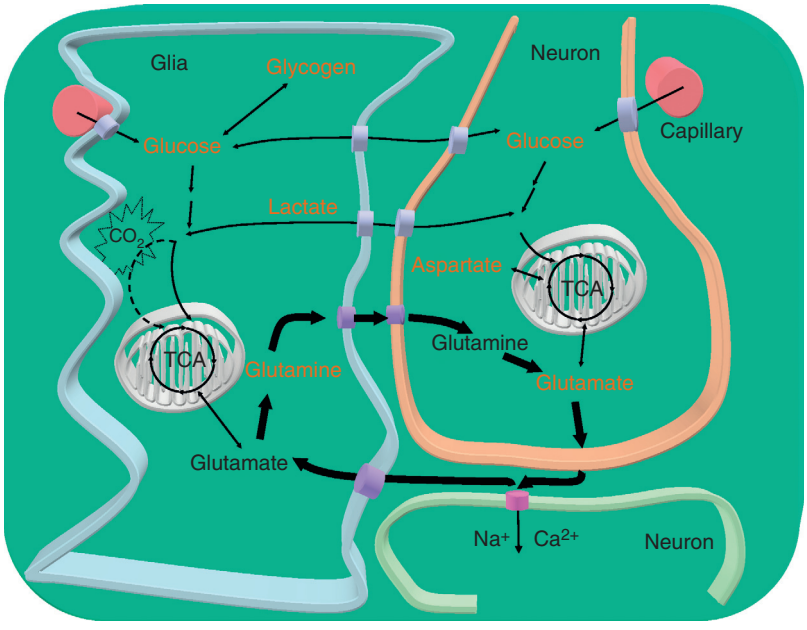

Figure 8 Schematic depiction of the metabolic relationship between neurons and glia. The compounds in red are those measured by nuclear magnetic resonance spectroscopy *in vivo*. Deactivation of neurotransmitter glutamate is primarily by uptake into the glia and conversion to glutamine, which at least in part diffuses back into the presynaptic terminal, to be converted to glutamate by phosphate-activated glutaminase, completing the glutamate–glutamine cycle (thick arrows; TCA, tricarboxcylic acid).

amino acids is thus a unique capability of the glial compartment, given that transamination which occurs in both astrocytes and neurons by itself cannot provide a net increase in tissue TCA cycle intermediate and hence amino acid concentration. In the reaction catalyzed by pyruvate carboxylase, pyruvate is combined with CO_2 to form oxaloacetate (OAA). As previously, we consider glucose labeled at the 1 and 6 positions as the precursor molecule, which results in label incorporation in the C3 of oxaloacetate from the C3 of pyruvate, which in turn labels the C2 of oxoglutarate, and thus the C2 of glutamate. As a result, the C2 of glutamate is labeled to a larger extent than is the C3. By comparing the labeling of glutamate in C2 and C3, the quantitative presence of anaplerotic reactions can be estimated *in vivo* by NMR, although some equilibrating flux back to fumarate may obscure the true extent of CO_2 fixation present. Anaplerotic reactions are a substantial metabolic activity in the brain, amounting to approximately one-third of glutamine synthesis, and are linked to brain activity. Anaplerotic reactions are decreased in metabolically depressed states, resulting in reduced glutamine synthesis and lowered brain glutamate and glutamine concentrations in hibernation, for example. Net synthesis of glutamine from glucose produces approximately ten ATPs per glutamine molecule, from the generation of several NADH molecules in the process, and thus is energetically favorable.

Summary

At rest, most of the energy requirements in the brain are matched by oxidative metabolism of glucose. Oxygen metabolism is uniquely compartmentalized between neurons and glia, the latter comprising about 25% of the energy metabolism. The consumption of acetate and fixation of CO_2 in glutamine are oxygen-dependent glial reactions. At least two-thirds of the ATP generated in astrocytes is by oxidative processes. Astrocytes thus can, in a unique way, buffer metabolic demand of the tripartite synapse. Glia exhibit a large capacity to phosphorylate glucose and can store it in the form of glycogen, the glucose equivalents of which can be exported in the form of lactate to neurons, providing neuroprotection. Astrocytes have a substantial anaplerotic activity, as *de novo* synthesis of glutamine by itself is an energetically favorable process. Glia therefore adapt the fuel demands to the specific requirements encountered in activation, hypoglycemia, and deactivation, nurturing surrounding neurons with substrates, while at the same time eliminating neurotransmitter glutamate from the synaptic cleft.

See also: Activity-Dependent Metabolism in Glia and Neurons; Glial Energy Metabolism: Overview; Glial Glycogen Metabolism; Glial Glutamate and GABA Metabolism; Glial Plasticity and Neuroendocrine Regulation; Glutamatergic and Gabaergic Systems; Magnetic Resonance Spectroscopy; Perfusion MRI.

Further Reading

Bouzier-Sore AK, Merle M, Magistretti PJ, et al. (2002) Feeding active neurons: (Re)emergence of a nursing role for astrocytes. *Journal of Physiology Paris* 96: 273–282.

Brown AM (2004) Brain glycogen re-awakened. *Journal of Neurochemistry* 89: 537–552.

Cerdan S, Rodrigues TB, Sierra A, et al. (2006) The redox switch/redox coupling hypothesis. *Neurochemistry International* 48: 523–530.

Gruetter R, Adriany G, Choi IY, et al. (2003) Localized *in vivo* ^{13}C NMR spectroscopy of the brain. *NMR in Biomedicine* 16: 313–338.

Gruetter R, Seaquist ER, and Ugurbil K (2001) A mathematical model of compartmentalized neurotransmitter metabolism in the human brain. *American Journal of Physiology (Endocrinology and Metabolism)* 281: E100–E112.

Hyder F, Patel AB, Gjedde A, et al. (2006) Neuronal–glial glucose oxidation and glutamatergic–GABAergic function. *Journal of Cerebral Blood Flow and Metabolism* 26: 865–877.

McKenna MC, Waagepetersen HS, Schousboe A, et al. (2006) Neuronal and astrocytic shuttle mechanisms for cytosolic-mitochondrial transfer of reducing equivalents: Current evidence and pharmacological tools. *Biochemical Pharmacology* 71: 399–407.

Morris P and Bachelard H (2003) Reflections on the application of ^{13}C-MRS to research on brain metabolism. *NMR in Biomedicine* 16: 303–312.

Oz G, Berkich DA, Henry PG, et al. (2004) Neuroglial metabolism in the awake rat brain: CO_2 fixation increases with brain activity. *Journal of Neuroscience* 24: 11273–11279.

Waagepetersen HS, Sonnewald U, and Schousboe A (2003) Compartmentation of glutamine, glutamate, and GABA metabolism in neurons and astrocytes: Functional implications. *Neuroscientist* 9: 398–403.

Zwingmann C and Leibfritz D (2003) Regulation of glial metabolism studied by 13C-NMR. *NMR in Biomedicine* 16: 370–399.